

A Journal of the Gesellschaft Deutscher Chemiker

Angewandte Chemie

GDCh

International Edition

www.angewandte.org

Accepted Article

Title: Direct NO Reduction by a Biomimetic Iron(II) Pyrazolate MOF

Authors: Zhongzheng Cai, Wenjie Tao, Curtis E. Moore, Shiyu Zhang, and Casey R. Wade

This manuscript has been accepted after peer review and appears as an Accepted Article online prior to editing, proofing, and formal publication of the final Version of Record (VoR). This work is currently citable by using the Digital Object Identifier (DOI) given below. The VoR will be published online in Early View as soon as possible and may be different to this Accepted Article as a result of editing. Readers should obtain the VoR from the journal website shown below when it is published to ensure accuracy of information. The authors are responsible for the content of this Accepted Article.

To be cited as: *Angew. Chem. Int. Ed.* 10.1002/anie.202108095

Link to VoR: <https://doi.org/10.1002/anie.202108095>

Direct NO Reduction by a Biomimetic Iron(II) Pyrazolate MOF

Zhongzheng Cai, Wenjie Tao, Curtis E. Moore, Shiyu Zhang, and Casey R. Wade*

[*] Dr. Z. Cai, Dr. W. Tao, Dr. C. E. Moore, Prof. Dr. S. Zhang, Prof. Dr. C. R. Wade
Department of Chemistry and Biochemistry
The Ohio State University
100 West 18th Ave, Columbus, OH 43210
E-mail: wade.521@osu.edu

Supporting information for this article is given via a link at the end of the document.

Abstract: A novel metal-organic framework (MOF) containing one-dimensional, Fe²⁺ chains bridged by dipyrazolate linkers and *N,N*-dimethylformamide (DMF) ligands has been synthesized. The unusual chain-type metal nodes feature accessible coordination sites on adjacent metal centers, resulting in motifs that are reminiscent of the active sites in non-heme diiron enzymes. The MOF facilitates direct reduction of nitric oxide (NO), producing nearly quantitative yields of nitrous oxide (N₂O) and emulating the reactivity of flavodiiron nitric oxide reductases (FNORs). The ferrous form of the MOF can be regenerated via a synthetic cycle involving reduction with cobaltocene (CoCp₂) followed by reaction with trimethylsilyl triflate (TMSOTf).

Metal-organic frameworks (MOFs) are promising platforms for the design of biomimetic materials.^[1–4] They are often assembled using linkers with weak-field donor groups such as carboxylates or azolates that are similar to those found in the active sites of metalloenzymes. MOF-supported reactive sites also benefit from site-isolation while the porous framework provides substrate access and a tunable microenvironment. However, metal-metal cooperativity, a key feature of multimetallic enzyme active sites, can be difficult to emulate in highly porous MOFs owing to the large spatial separation between reactive structural components. In this regard, MOFs assembled from secondary building units (SBUs) comprised of one-dimensional metal chains are potentially well-equipped to facilitate cooperative substrate activation at adjacent metal sites and enable multi-electron processes by distributing the metal redox burden. However, reported examples of cooperative and multi-electron reactivity in MOFs with chain-type SBUs remain rare, in part due to their tendency to contain coordinatively saturated metal sites.^[5,6]

Nitric oxide (NO) acts a critical signaling molecule in biological systems, but becomes toxic at elevated concentrations.^[7,8] Flavodiiron nitric oxide reductases (FNORs) are a family of enzymes found in pathogenic bacteria that reduce NO to nontoxic N₂O as a protective mechanism.^[9,10] The FNOR active site consists of a non-heme diiron cluster (Fe–Fe distance of 3.2–3.6 Å) coordinated by histidine and carboxylate ligands, and several model complexes have been designed to investigate its NO reduction mechanism.^[11–13] Recently, Lehnert and coworkers reported the only example of a diferrous, non-heme model complex capable of reducing NO to N₂O via N–N bond coupling between {FeNO}⁷ groups.^[14,15] Prior to this report, {FeNO}⁷ species were

generally considered too stable to promote direct NO reduction, although a ferrous NO reduction pathway has been demonstrated for flavodiiron proteins.^[16–18]

In contrast to small molecule complexes, the biomimetic reactivity of iron-based MOFs toward NO has not been thoroughly explored.^[2,4] Coordinatively unsaturated iron sites in MIL-88(Fe), MIL-101(Fe), and Fe₂(dobdc) have been shown to exhibit strong and reversible interactions with NO (Figure 1a).^[19–21] In addition, Fe²⁺-exchanged MOF-5 and Cu^I-MFU-4l have been found to mediate NO disproportionation to generate M–NO₂ species and N₂O (Figure 1b).^[22–24] Unlike FNORs, in which the diiron active site is poised to facilitate N–N bond coupling, the isolated Fe²⁺ and Cu^I sites at the SBUs of these MOFs are incapable of direct, two-electron reduction of NO.

Here, we report the synthesis and NO reduction reactivity of a Fe²⁺-pyrazolate MOF (**1**) featuring chain-type SBUs with accessible coordination sites on adjacent Fe²⁺ centers. These motifs resemble the active sites of non-heme diiron enzymes, such as FNORs, that use cooperative substrate activation to carry out multielectron redox processes. **1** generates N₂O in nearly quantitative yield upon exposure to stoichiometric amounts of NO, emulating the reactivity of FNORs and representing a rare example of direct NO reduction from ferrous sites (Figure 1c). Moreover, sequential reaction of the oxidized MOF product with a reductant and Lewis acid regenerates the Fe²⁺ form of the MOF, which maintains NO reduction activity.

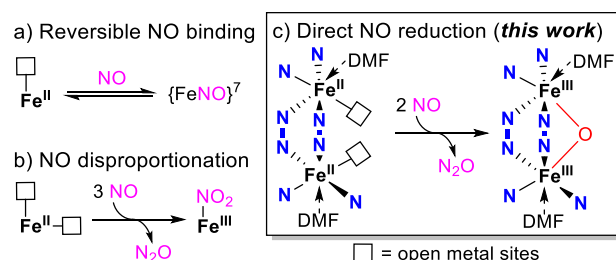


Figure 1. Reactivity of iron-based MOFs with NO.

Solvothermal reaction of Fe(OTf)₂(THF)₂ (OTf = triflate, THF = tetrahydrofuran) and H₂bppdi (2,6-bis(1H-pyrazolyl)pyromellitic diimide) in the presence of triethylamine generates **1** as an orange, microcrystalline powder after washing with DMF and THF (Figure 2a). Solid **1** rapidly oxidizes upon exposure to air, as indicated by a

COMMUNICATION

color change from orange to bright red, and gradually decomposes under ambient conditions. ^1H NMR spectra of acid-digested samples of **1** show a $\text{H}_2\text{bppdi}:\text{DMF}:\text{THF}$ ratio of 1:0.5:3, which supports an empirical formula of $\text{Fe}(\text{bppdi})(\text{DMF})_{0.5}(\text{THF})_3$ (Figure S2). Zero-field, ^{57}Fe Mössbauer spectroscopy was used to investigate the metal oxidation state in **1** (Figure 4a, see Supporting Information for additional details). The spectrum measured at 4 K displays a broad quadrupole doublet with an isomer shift (δ) of 1.09 mm/s and quadrupole splitting parameter (ΔE_Q) of 3.01 mm/s that corresponds to the presence of high-spin iron(II) species. The broad absorption signal suggests some variability in the metal coordination environment, which has been observed for other iron-based MOFs and proposed to arise from framework distortions or differences in solvent coordination.^[25,26]

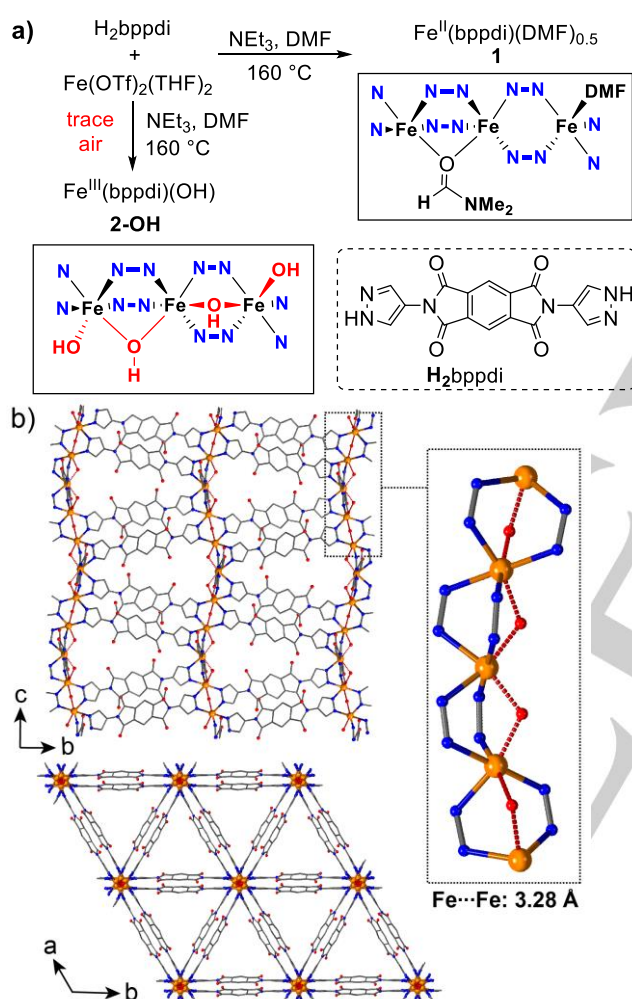


Figure 2. a) Synthesis of **1** and **2-OH**. b) Single crystal structure of **2-OH**.

Although we have been unable to obtain a single crystal of **1** suitable for X-ray diffraction, the framework structure has been established from single crystals of an oxidized Fe^{3+} analogue, **2-OH** (Figure 2b).^[27] A few small red crystals of the latter were obtained during reaction optimization, with oxidation attributed to the presence of adventitious $\text{O}_2/\text{H}_2\text{O}$. **2-OH** crystallizes in the $P6_1$ space group with helical, chain-type SBUs linked by the linear dipyrazolates to form triangular channels ~ 10 Å in diameter. Each Fe^{3+} center adopts a pseudo-octahedral geometry via coordination of four different pyrazolate units and two

$\mu\text{-OH}$ ligands. Notably, the $\text{Fe}\cdots\text{Fe}$ distance between adjacent metal sites (3.28 Å) is similar to that found in the diiron active site of FNORs (3.2–3.6 Å).^[28] The framework structure of **2-OH** is reminiscent of $\text{Fe}_2(\text{bdp})_3$ ($\text{bdp}^{2-} = 1,4\text{-benzenedipyrazolate}$).^[29,30] However, while $\text{Fe}_2(\text{bdp})_3$ contains octahedral Fe^{3+} centers coordinated by six pyrazolate linkers, each Fe^{3+} site in **2-OH** is only 4-connected with $\mu\text{-hydroxide}$ ligands replacing an absent dipyrazolate linker. Moreover, **2-OH** is quite unique in that the $\mu\text{-hydroxide}$ groups bridging adjacent pairs of atoms are mutually *cis*, resulting in a disphenoidal arrangement of pyrazolate N donors and the formation of helical chains.^[31]

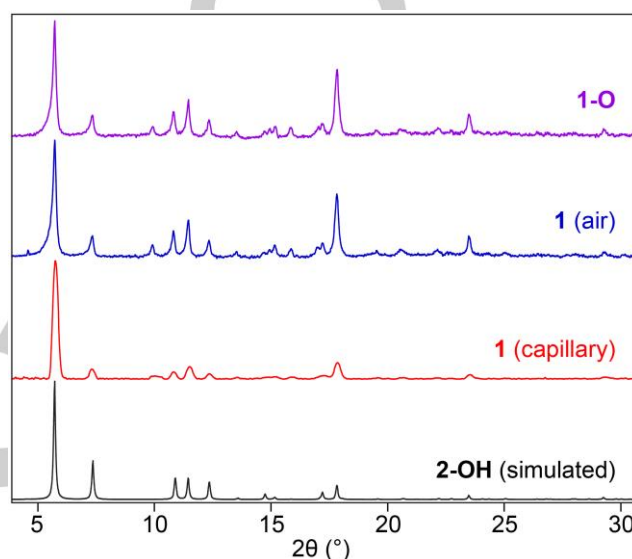


Figure 3. PXRD patterns of **1** measured under air-free conditions in a sealed capillary and upon exposure to air along with the pattern of **1-O** and that simulated from the single crystal structure of **2-OH**.

The powder X-ray diffraction (PXRD) pattern of **1** matches that simulated from the single-crystal structure of **2-OH**, confirming that the MOFs adopt similar framework structures (Figure 3). However, the presence of Fe^{2+} centers in **1** requires coordination of neutral bridging ligands at the chain-type SBUs rather than the $\mu\text{-hydroxide}$ groups found in **2-OH**. ^1H NMR and TGA analysis of **1** show a 2:1 $\text{H}_2\text{bppdi}:\text{DMF}$ ratio (Figures S3 and S6), and the redshifted DMF $\nu(\text{CO})$ band observed in the IR spectrum signals its coordination to a metal (Figure S4).^[32] Together these data indicate that DMF solvent molecules act as bridging ligands in the chain-type SBUs. The 2:1 linker:DMF ratio also suggests that the DMF ligands only occupy half of the bridging coordination sites. Consequently, the coordination sites between alternating pairs of Fe^{2+} sites along the chain-type SBUs should remain open or occupied by weakly coordinating THF molecules. **1** was gently activated by heating at 60 °C under vacuum (10^{-4} bar), and a subsequent N_2 adsorption isotherm (77 K) gave a calculated Brunauer-Emmett-Teller (BET) surface area of $1330 \text{ m}^2 \text{ g}^{-1}$ (Figure S5). The acid-digested ^1H NMR spectrum of the activated sample shows that the $\text{H}_2\text{bppdi}:\text{DMF}$ ratio is largely unchanged, further supporting the role of DMF as a bridging ligand (Figure S6). Subsequent attempts to activate **1** at higher temperatures resulted in volatilization of the bridging DMF molecules and framework collapse (Figure S7 and S8). This behavior

COMMUNICATION

clearly indicates that the DMF molecules provide necessary structural support.

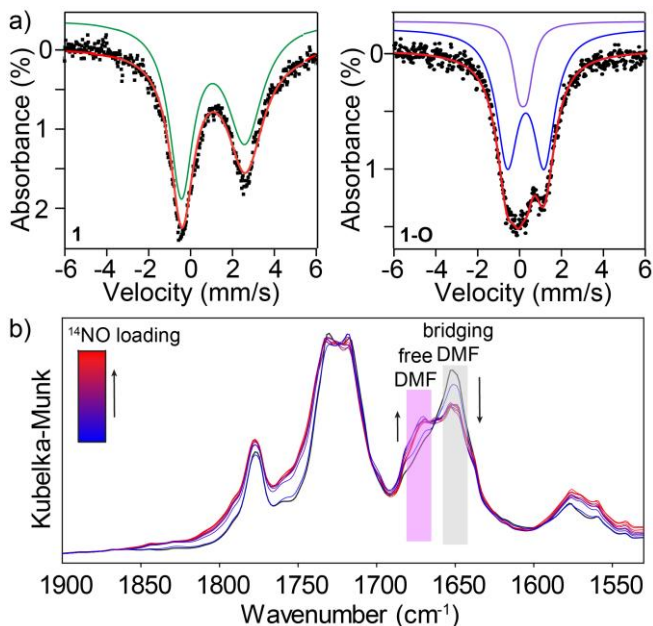
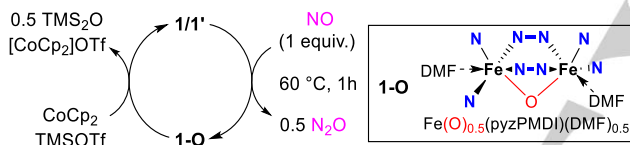


Figure 4. a) ⁵⁷Fe Mössbauer spectra (4 K) of **1** and **1-O**. b) Room temperature DRIFTS spectra measured for **1** upon exposure to dilute ¹⁴NO (~25% vol).

Scheme 1. Synthetic cycle for reaction of **1** with NO and regeneration of **1'**.



Motivated by the resemblance of the putative ferrous diiron motifs in **1** to the FNOR active site, we set out to investigate its reactivity toward NO (Scheme 1). Solid **1** undergoes an immediate color change from orange to black upon exposure to 1.0 equiv. of NO gas per Fe²⁺ in a sealed vial at room temperature. The black solid gradually turns to red when left at ambient temperature, but the color change could be accelerated with mild heating. GC analysis of the headspace 1 min after the addition of NO revealed formation of N₂O in 27 % yield (Figure S42). N₂O production gradually increased over time, reaching 60 % yield in the headspace after 1 h. Nearly quantitative N₂O yields (91-99%, Table S2) were obtained for multiple batches of **1** when the reaction was heated at 60 °C for 1 h and N₂O adsorption by the MOF was taken into account (see Supporting Information for details). In situ diffuse reflectance infrared Fourier transform spectroscopy (DRIFTS) experiments were carried out by dosing **1** with dilute NO or isotopically labeled ¹⁵NO (Figure 3b and S9). Some minor intensity changes are observed in the 1700-1750 cm⁻¹ region where the NO stretch of {Fe(NO)}⁷ species might be expected to appear, but comparison of the difference spectra do not clearly reveal the buildup of any intermediates (Figure S10). The DRIFT spectra do show a shift in intensity of the bridging DMF ν(CO) band from 1652 cm⁻¹ to 1675 cm⁻¹. This shift is consistent with solvent decoordination, insinuating reaction of NO at the Fe²⁺ sites.^[32] Notably, a DMSO solvent-exchanged analogue (**1-DMSO**) shows NO reduction activity

comparable to **1**, but similar features are not observed in the 1600-1700 cm⁻¹ region of its DRIFT spectra upon exposure to NO, confirming their assignment as DMF ν(CO) bands (Figures S12 and S33).

The N₂O yield drops significantly when **1** is treated with excess NO. Reaction with 2 equiv. of NO per Fe²⁺ afforded only 67 % N₂O yield after heating at 60 °C for 2 h. GC monitoring of the reaction of **1** with 3 equiv. of NO revealed even greater inhibition, with less than 10 % N₂O yield observed over the course of 1 h at room temperature. The IR spectrum of **1** upon exposure to 5 equiv. of NO (**1-exNO**) shows the appearance of broad ν(NO) bands around 1851 and 1832 cm⁻¹ as well as a new feature at 1573 cm⁻¹ (Figure S13). These new signals redshift by 25-50 cm⁻¹ when ¹⁵NO is used, confirming their association with NO-derived species (Figure S14). The frequency of the ν(NO) bands is unusually high for {FeNO}⁷ species and indicates the presence of weakly activated NO ligands.^[11,33,34] On the other hand, the band at 1573 cm⁻¹ appears below the typical N–O stretching region for mono-nitrosyl complexes. It is reminiscent of ν(NO) bands observed for diiron μ-nitrosyl species, but such an assignment is tenuous given that the Fe...Fe distances in **2-OH** (3.28 Å) are significantly longer than those found in structurally characterized μ-nitrosyl complexes (2.4-2.6 Å).^[35,36] Moreover, the band is inconsistent with hyponitrite (–O–N=N–O–) or nitro/nitrito (NO₂⁻) groups which typically exhibit N–O and N=N stretching bands at lower frequencies.^[37,38] Although the identity of the species formed upon reaction of **1** with excess NO remains ambiguous, the dramatic decrease in reactivity supports a direct reduction rather than disproportionation mechanism since the latter should be promoted by increasing NO concentration.^[22,23] This behavior also suggests that key N–N coupling or N₂O release steps may be inhibited by binding of excess NO at the Fe²⁺ sites. Several plausible mechanisms have been proposed for N–N coupling in diiron proteins and model complexes (Figure S15).^[9,18] Among these, there is strong evidence that supports a pathway involving diferrous dinitrosyl intermediates.^[17,39] In the case of **1**, a similar diferrous dinitrosyl pathway seems feasible given the short the Fe...Fe distances the accessibility of coplanar coordination sites. However, the present data preclude distinction among the mechanistic possibilities, and more detailed kinetic and computational studies will be needed to interrogate the mechanism operative for **1**.

The oxidized MOF product, **1-O**, maintains crystallinity and exhibits a BET surface area of 1110 m²g⁻¹, only slightly lower than that of **1** (Figure S5). The IR spectrum shows no indication of residual Fe–NO species or Fe–NO₂ groups that would result from NO disproportionation (Figure S18). The ⁵⁷Fe Mössbauer spectrum exhibits a broad signal that could be fitted as two overlapping doublets (79 %, δ₁ = 0.36 mm/s, ΔE_{Q1} = 1.78 mm/s and 21 %, δ₂ = 0.23 mm/s, ΔE_{Q2} = 0.40 mm/s, Figure 4a). Again, the broad absorption profile observed for this material suggests a distribution of slightly different local coordination environments.^[25,26] The isomer shifts of both components are characteristic of Fe³⁺ and consistent with data reported for oxo-bridged complexes.^[40] The appearance of two distinct Fe³⁺ sites may be related to the partial release of coordinated DMF solvent molecules upon reaction with NO. Nevertheless, these data support direct reduction of NO to N₂O with

COMMUNICATION

concomitant formation of $\text{Fe}^{3+}\text{-O-Fe}^{3+}$ species at the chain-type SBUs of **1-O**.

Lastly, we sought to determine if the active Fe^{2+} form of the MOF could be regenerated from **1-O**. To this end, cobaltocene (CoCp_2) was employed as a reductant and trimethylsilyl triflate (TMSOTf) as an oxide abstracting reagent (Scheme 1). **1-O** was initially treated with CoCp_2 in acetonitrile (MeCN), resulting in formation of **1-CoCp₂** as a green solid. ^1H NMR analysis of an acid-digested sample of **1-CoCp₂** after extensive washing shows a 1:1 $\text{H}_2\text{bppdi}:[\text{CoCp}_2]^+$ ratio, consistent with one-electron reduction per formula unit (i.e. $[\text{CoCp}_2]^+[\text{Fe}(\text{bppdi})(\text{O})_{0.5}]^-$, Figure S21). The ^{57}Fe Mössbauer and X-ray photoelectron spectra corroborate metal-based reduction to form Fe^{2+} intermediate species (Figures S22 and S30). Subsequent addition of TMSOTf to **1-CoCp₂** affords **1'** as an orange solid that closely resembles **1**. PXRD and N_2 adsorption measurements show that the MOF maintains crystallinity and porosity while the acid-digested ^1H NMR spectrum confirms the complete departure of $[\text{CoCp}_2]^+$ from the framework (Figures S24-S26). The ^{57}Fe Mössbauer spectrum of **1'** exhibits a quadrupole doublet ($\delta = 1.04 \text{ mm s}^{-1}$ and $\Delta E_Q = 3.07 \text{ mm/s}$) that matches the signal observed for **1** (Figure S31). Gratifyingly, reaction of **1'** with 1 equiv. NO under the same conditions employed for **1** produced N_2O in 73% yield (Figure S37), confirming successful regeneration of the active Fe^{2+} species with only a modest decrease in activity. Unfortunately, CoCp_2 is not directly compatible with NO, precluding investigation of catalytic NO reduction with this combination of reagents.^[41] Nevertheless, this synthetic cycle illustrates the potential of **1** to be exploited for catalytic small molecule activation and further studies in this area are ongoing.

In summary, we report the synthesis and unprecedented biomimetic reactivity of a novel Fe^{2+} pyrazolate MOF. The unusual chain-type SBUs in **1** facilitate direct reduction of NO from the ferrous state, which is a rare mode of reactivity for FNOR model complexes.^[14] Moreover, **1** can be regenerated via a synthetic cycle involving sequential treatment with a mild reductant and oxide abstracting reagent. These findings endorse further investigation of chain-type MOFs as a means of mimicking cooperative, multi-electron reactivity found in metalloenzymes.

Acknowledgements

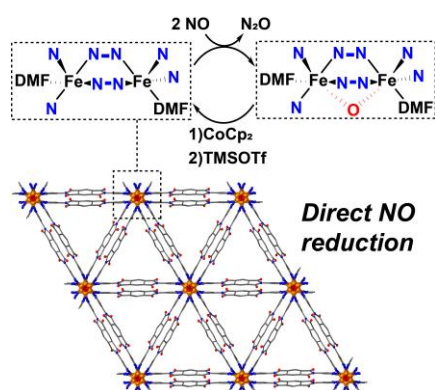
This work was supported by an Early Career Faculty grant (80NSSC18K1504) from the NASA Space Technology Research Grants Program. The authors acknowledge the Surface Analysis Laboratory (NSF DMR-0114098) of the Ohio State University Department of Chemistry and Biochemistry. We also thank Tom Rayder and Jordan Hilliard for assistance with gas adsorption measurements.

Keywords: Bioinspired materials • Metal-organic frameworks • Nitric oxide

- [1] I. Nath, J. Chakraborty, F. Verpoort, *Chem. Soc. Rev.* **2016**, *45*, 4127–4170.
- [2] X. Liu, Y. Zhou, J. Zhang, L. Tang, L. Luo, G. Zeng, *ACS Appl. Mater. Interfaces* **2017**, *9*, 20255–20275.
- [3] K. Chen, C.-D. Wu, *Coord. Chem. Rev.* **2019**, *378*, 445–465.
- [4] J. R. Bour, A. M. Wright, X. He, M. Dincă, *Chem. Sci.* **2020**, *11*, 1728–1737.
- [5] D. Y. Osadchii, A. I. Olivos-Suarez, Á. Szécsényi, G. Li, M. A. Nasalevich, I. A. Dugulan, P. S. Crespo, E. J. M. Hensen, S. L. Veber, M. V. Fedin, G. Sankar, E. A. Pidko, J. Gascon, *ACS Catal.* **2018**, *8*, 5542–5548.
- [6] Á. Szécsényi, G. Li, J. Gascon, E. A. Pidko, *Chem. Sci.* **2018**, *9*, 6765–6773.
- [7] T. Nagano, T. Yoshimura, *Chem. Rev.* **2002**, *102*, 1235–1270.
- [8] A. W. Carpenter, M. H. Schoenfish, *Chem. Soc. Rev.* **2012**, *41*, 3742.
- [9] J. Kurtz Donald M., *Dalton Trans.* **2007**, 4115–4121.
- [10] S. Khatua, A. Majumdar, *J. Inorg. Biochem.* **2015**, *142*, 145–153.
- [11] T. C. Berto, A. L. Speelman, S. Zheng, N. Lehnert, *Coord. Chem. Rev.* **2013**, *257*, 244–259.
- [12] N. Lehnert, K. Fujisawa, S. Camarena, H. T. Dong, C. J. White, *ACS Catal.* **2019**, *9*, 10499–10518.
- [13] M. Jana, C. J. White, N. Pal, S. Demeshko, C. Cordes (née Kupper), F. Meyer, N. Lehnert, A. Majumdar, *J. Am. Chem. Soc.* **2020**, *142*, 6600–6616.
- [14] H. T. Dong, C. J. White, B. Zhang, C. Krebs, N. Lehnert, *J. Am. Chem. Soc.* **2018**, *140*, 13429–13440.
- [15] $(\text{FeNO})^7$ is the Enemark–Feltham notation for ferrous-nitrosyl. See: J. H. Enemark, R. D. Feltham, *Coord. Chem. Rev.* **1974**, *13*, 339–406.
- [16] T. Hayashi, J. D. Caranto, D. A. Wampler, D. M. Kurtz, P. Moëne-Loccoz, *Biochemistry* **2010**, *49*, 7040–7049.
- [17] J. D. Caranto, A. Weitz, N. Giri, M. P. Hendrich, D. M. Kurtz, *Biochemistry* **2014**, *53*, 5631–5637.
- [18] J. D. Caranto, A. Weitz, M. P. Hendrich, D. M. Kurtz, *J. Am. Chem. Soc.* **2014**, *136*, 7981–7992.
- [19] A. C. McKinlay, J. F. Eubank, S. Wuttke, B. Xiao, P. S. Wheatley, P. Bazin, J.-C. Lavalley, M. Daturi, A. Vimont, G. De Weireld, P. Horcajada, C. Serre, R. E. Morris, *Chem. Mater.* **2013**, *25*, 1592–1599.
- [20] J. F. Eubank, P. S. Wheatley, G. Lebars, A. C. McKinlay, H. Leclerc, P. Horcajada, M. Daturi, A. Vimont, R. E. Morris, C. Serre, *APL Mater.* **2014**, *2*, 124112.
- [21] E. D. Bloch, W. L. Queen, S. Chavan, P. S. Wheatley, J. M. Zadrozny, R. Morris, C. M. Brown, C. Lamberti, S. Bordiga, J. R. Long, *J. Am. Chem. Soc.* **2015**, *137*, 3466–3469.
- [22] C. K. Brozek, J. T. Miller, S. A. Stoian, M. Dincă, *J. Am. Chem. Soc.* **2015**, *137*, 7495–7501.
- [23] J. Jover, C. K. Brozek, M. Dincă, N. López, *Chem. Mater.* **2019**, *31*, 8875–8885.
- [24] A. M. Wright, C. Sun, M. Dincă, *J. Am. Chem. Soc.* **2021**, *143*, 681–686.
- [25] K. Sumida, S. Horike, S. S. Kaye, Z. R. Herm, W. L. Queen, C. M. Brown, F. Grandjean, G. J. Long, A. Dailly, J. R. Long, *Chem. Sci.* **2010**, *1*, 184–191.
- [26] A. Jaffe, M. E. Ziebel, D. M. Halat, N. Biggins, R. A. Murphy, K. Chakarawet, J. A. Reimer, J. R. Long, *J. Am. Chem. Soc.* **2020**, *142*, 14627–14637.
- [27] CCDC 2054298 (**2-OH**) contains the supplementary crystallographic data for this paper. These data can be obtained free of charge from The Cambridge Crystallographic Data Centre.
- [28] R. Silaghi-Dumitrescu, D. M. Kurtz, L. G. Ljungdahl, W. N. Lanzilotta, *Biochemistry* **2005**, *44*, 6492–6501.
- [29] Z. R. Herm, M. M. Wiers, J. A. Mason, J. M. van Baten, M. R. Hudson, P. Zajdel, C. M. Brown, N. Masciocchi, R. Krishna, J. R. Long, *Science* **2013**, *340*, 960–964.
- [30] N. Biggins, M. E. Ziebel, M. I. Gonzalez, J. R. Long, *Chem. Sci.* **2020**, *11*, 9173–9180.
- [31] Y.-J. Qi, Y.-J. Wang, X.-X. Li, D. Zhao, Y.-Q. Sun, S.-T. Zheng, *Cryst. Growth Des.* **2018**, *18*, 7383–7390.
- [32] K. I. Hadjiivanov, D. A. Panayotov, M. Y. Mihaylov, E. Z. Ivanova, K. K. Chakarova, S. M. Andonova, N. L. Drenchev, *Chem. Rev.* **2020**, *acs.chemrev.0c00487*.
- [33] J. A. McCleverty, *Chem. Rev.* **2004**, *104*, 403–418.
- [34] J. Li, A. Banerjee, P. L. Pawlak, W. W. Brennessel, F. A. Chavez, *Inorg. Chem.* **2014**, *53*, 5414–5416.
- [35] K. D. Karlin, D. L. Lewis, H. N. Rabinowitz, S. J. Lippard, *J. Am. Chem. Soc.* **1974**, *96*, 6519–6521.
- [36] S. I. Källäne, A. W. Hahn, T. Weyhermüller, E. Bill, F. Neese, S. DeBeer, M. van Gastel, *Inorg. Chem.* **2019**, *58*, 5111–5125.
- [37] A. M. Wright, T. W. Hayton, *Inorg. Chem.* **2015**, *54*, 9330–9341.
- [38] K. Nakamoto, *Infrared and Raman Spectra of Inorganic and Coordination Compounds, Part B*, John Wiley & Sons, Inc., Hoboken, NJ, USA, **2008**.
- [39] C. Van Stappen, N. Lehnert, *Inorg. Chem.* **2018**, *57*, 4252–4269.
- [40] D. M. Kurtz, *Chem. Rev.* **1990**, *90*, 585–606.
- [41] R. S. Hay-Motherwell, G. Wilkinson, T. K. N. Sweet, M. B. Hursthouse, *J. Chem. Soc., Dalt. Trans.* **1994**, 2223–2232.

COMMUNICATION

Entry for the Table of Contents



A novel iron(II) MOF containing accessible coordination sites on adjacent metal centers facilitates the direct reduction of NO to N₂O.